doi:10.2533/chimia.2025.228 Chimia 79 (2025) 228–231

Metal Oxides of Group 4: General Insights and the Synthesis of ZrO_2/HfO_2 and ZrO_2:Eu/ZrO_2 Core/Shell Nanocrystals

Carlotta Seno[§*]

[§]SCS-Metrohm Award for best oral presentation in Materials Chemistry

Abstract: Metal oxide nanocrystals, like ZrO_2 and HfO_2, serve as hosts for optically active lanthanide ions. However, synthesizing colloidally stable nanocrystals with complex architectures remains challenging. We have pioneered the synthesis of metal oxide core/shell nanocrystals, where HfO_2 epitaxially grows onto ZrO_2. The beneficial effect of the shell on the optical properties is demonstrated by investigating the photoluminescence of ZrO_2:Eu and of ZrO_2:Eu/ZrO_2 after growing a protective zirconia shell on it.[1]

Keywords: Core/Shell · Lifetime · Metal Oxides · Nanoparticles · Photoluminescence

Carlotta Seno obtained her Bachelor and Master degrees in chemistry at ETH Zurich. During her master's thesis under Prof. Markus Niederberger and Prof. André Studart, she studied the triboluminescence in manganese-doped zinc sulfide nanoparticles. In 2021 she started her PhD under the supervision of Prof. Jonathan De Roo at the University of Basel. She is working on the synthesis and characterization of complex oxide nanocrystals. During this time, she spent 4 months in the group of Prof. Simon Billinge at Columbia University to improve her knowledge of the characterization technique Pair Distribution Function.

1. Introduction: Metal Oxides of Group 4

Titania (TiO_2), zirconia (ZrO_2), and hafnia (HfO_2) (Fig. 1) form an interesting class of nanomaterials, with many properties and applications. While these materials share several chemical and physical characteristics, zirconium and hafnium are often referred to as *twin metals* due to their similarities. In contrast, titanium, although chemically related, often behaves somewhat differently.[2] The three oxides exhibit high thermal and chemical stability,[3–5] and biocompatibility. These properties, combined with their electronic, optical, and structural characteristics have enabled their use in various advanced applications. The high dielectric constants of these oxides[2] make them ideal for applications in capacitors, gate insulators for semiconductor devices, and energy storage systems. Zirconia nanocrystals are components for (in)-organic composites[2,6–8] while hafnia nanocrystals have found utility in memory devices.[9,10] Their high refractive indices[3] make these materials valuable in optical coatings for lenses, mirrors, and display technologies.[3,11,12] Titania, with a band gap of approximately 3 eV, absorbs blue and UV light, while zirconia and hafnia, with band gaps around 5.8 eV, function deep in the UV range. Titania's smaller band gap makes it a leading material for photocatalysts[13,14] and photovoltaics.[15–17] In nanocomposites made of nanocrystals, dyes, and polymers, hafnia absorbs photons and transfers them to a cascade of dyes, converting them to visible light.[2] The large band gap of these three metal oxides is a key factor in their ability to host dopants. When doped with tantalum (Ta^{5+}) or niobium (Nb^{5+}), the optoelectronic properties of titania are changed, as free electrons are introduced in its conduction band, enabling infrared plasmon resonance.[18,19] When lanthanide ions are used as dopants, all three metal oxides are useful in applications as luminescent materials.[20–23]

Fig. 1. Glimpse of the periodic table of the elements highlighting the three metals of group 4.

1.1 *Zr and Hf: Not Always Twin Metals*

Despite their significant difference in atomic mass, zirconium, and hafnium exhibit almost identical atomic radii: 0.83 Å for Hf^{4+} and 0.84 Å for Zr^{4+}.[2] Consequently, zirconia and hafnia are isomorphous in every phase, which means they share crystal structures with very similar lattice parameters. As a result, it is possible to form a series of solid solutions of $Hf_xZr_{1-x}O_2$ in the bulk, where $0.11 < x < 0.84$.[24] This is not the case for $HfTiO_2$ and $ZrTiO_2$ which were not possible to obtain because of the different reactivities of Hf and Zr compared to Ti.[24] Although zirconium and hafnium are referred to as *twin metals*, their oxides do not consistently adopt the same structure under identical synthesis conditions.[25,26] For example, when metal chloride and metal isopropoxide precursors are mixed in tri-*n*-octylphosphine oxide (TOPO) and heated up to 340 °C for 2 hours, zirconia nanoparticles crystallize in the tetragonal phase, while hafnia nano-

*Correspondence: C. Seno, E-mail: carlotta.seno@unibas.ch
Department of Chemistry, University of Basel, CH-4058 Basel.

particles form in the monoclinic phase. This structural difference also impacts their morphology, with zirconia forming spherical nanoparticles and hafnia yielding rod-shaped nanoparticles.[25,26] The difficulty in stabilizing tetragonal hafnia arises from its significantly smaller critical size for stabilization compared to zirconia (4 nm versus 30 nm).[27] This divergence is due to a stronger driving force for the stabilization of the monoclinic phase in hafnia compared to zirconia. In fact, the difference in bulk free energies ($\Delta G_{bulk,\ monoclinic} - \Delta G_{bulk,\ tetragonal}$) is approximately 40% bigger for HfO_2 compared to ZrO_2 (–196 meV versus –140 meV).[27–29] Additionally, the smaller volume expansion associated with the martensitic tetragonal-to-monoclinic transformation in hafnia (2.7% versus at least 4% for zirconia) reduces the elastic strain energy required for the phase transition.[27] Finally, the tetragonal-to-monoclinic phase transformation enthalpy of HfO_2 is 75% higher than that of ZrO_2, which implies less stringent conditions for it to occur in hafnia compared to zirconia.[26]

1.2 *Surfactant Assisted Synthesis in TOPO*

Non-aqueous surfactant-assisted syntheses enable the formation of nanoparticles with high crystallinity, monodispersity, and colloidal stability.[2] In the case of metal oxides of group 4, the reaction of metal alkoxide with metal halide in TOPO has been widely used and studied, in particular for zirconium and hafnium.[24,27,30–33] At the end of the reaction (after 2 hours at 340 °C), and after purification, the nanoparticles are covered and stabilized by a mixture of protonated TOPO, dioctyl phosphinate, and dioctyl pyrophosphonate.[34] ZrO_2 is obtained as 4-nm tetragonal spheres, while hafnia as monoclinic rod-shaped nanoparticles. However, the synthesis of colloidal group 4 metal oxide nanocrystals presents many challenges, and achieving synthetic control over the final properties of the nanoparticles remains difficult. Size control is limited to 3 to 5.5 nm,[30–32] with little control over architectures, like core/shells, alloys, or mixed phase nanoparticles.

1.3 *The Core/Shell Architecture*

Core/shell structures are a type of heterostructure extensively explored in the field of quantum dots.[35] It has been shown that covering an optically active core with a protecting layer improves the quantum efficiency of the core. In fact, the protective layer can prevent surface quenching, a process where excited electrons and holes interact with surface defects or traps, leading to non-radiative recombination and the loss of photon emission. The shell suppresses non-radiative processes that are responsible for decreasing quantum efficiency.

Despite zirconia and hafnia being suitable host materials for dopants like europium, the core/shell architecture for these materials remains unexplored. The goal, therefore, was to create a shell around europium-doped zirconia with a protective layer of pure zirconia.

2. Core/Shell Synthesis and Optical Properties[1]

2.1 *Method Development with ZrO_2/HfO_2*

In our recent publication,[1] we first optimized the method by shelling spherical zirconia with a shell of hafnia. Using the same

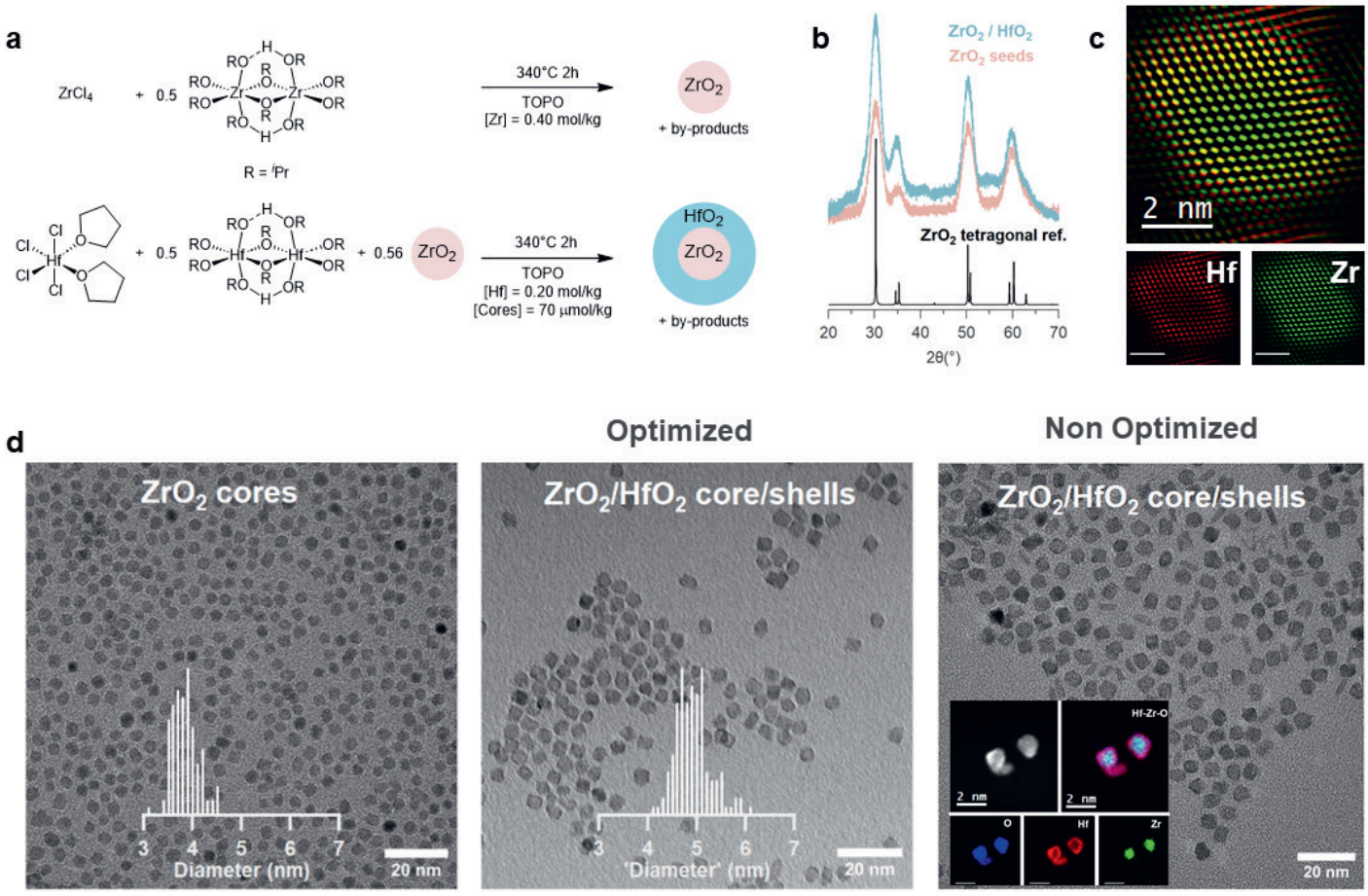

Fig. 2. a) Synthetic procedures to obtain ZrO_2 and ZrO_2/HfO_2 core/shell nanocrystals, where the metal chloride, isopropanol, tetrahydrofuran, and propene are obtained as by-products, b) powder XRD spectra of ZrO_2 cores and ZrO_2/HfO_2 core/shell, c) frequency-filtered map HAADF STEM image of ZrO_2/HfO_2 core/shell, d) bright-field TEM images of ZrO_2 cores, ZrO_2/HfO_2 core/shells after synthesis optimization, and ZrO_2/HfO_2 before optimization, with the insert showing high-angle annular dark-field (HAADF) scanning TEM and the corresponding EDX compositional maps. The histograms are based on more than 100 particles. Reprinted with permission from ref. [1].

synthesis conditions, spheres of zirconia and rods of hafnia can be produced. This allows us to distinguish by transmission electron microscopy (TEM) whether hafnia grows on the existing zirconia cores, making them bigger, or nucleates independently forming rods. So, zirconia nanoparticles were synthesized, and after purification, they were mixed with hafnium chloride and hafnium isopropoxide precursors in TOPO (Fig. 2a) Powder X-ray diffraction (XRD) spectra (Fig. 2b) shows that the peaks of the core/shell are narrower compared to the starting zirconia cores, indicating particle growth. Furthermore, the XRD spectrum after shelling shows a tetragonal crystal phase suggesting epitaxial growth of hafnia on zirconia. High-resolution TEM in Fig. 2c confirms the core/shell structure, showing zirconium in green confined to the centre and hafnium, in red, in the shell. This is further indicated in the bright-field TEM images (Fig. 2d). The initial zirconia cores have a diameter of 3.8 nm, while the nanoparticles after shelling grew to 4.9 nm. Before synthesis optimization, the TEM image shows the presence of both larger particles as well as numerous rods, which were confirmed to be pure hafnia using energy-dispersive X-ray spectroscopy (EDX) compositional mapping. After optimization, secondary nucleation of hafnia is suppressed, giving the desired particles.

2.2 *Shelling of ZrO_2:Eu and its Optical Properties*

With the method established, we proceeded to synthesize our target structure.[1] Europium-doped zirconia nanoparticles (10.0% nominal doping) were first synthesized in an autoclave and then functionalized with dodecanoic acid (Fig. 3a). These particles were subsequently mixed with zirconium chloride and zirconium isopropoxide precursors in TOPO and reacted at 340 °C for 2 hours.

The particle size increased from an initial diameter of 3.5 nm to 5.1 nm, which was determined by measuring the projected area of the faceted nanocrystals and calculating the diameter from the bright-field TEM images shown in Fig. 3b (same procedure used to obtain the diameter of ZrO_2/HfO_2 nanoparticles in section 2.1).

Finally, we investigated the optical properties of europium before and after shelling using photoluminescence emission spectroscopy.[1] Upon shelling, certain emission channels disappear, leading to an emission spectrum with narrower peaks (Fig. 3c). This suggests a change in the coordination around the europium to a more uniform environment. The shell also significantly impacts the lifetime of the excited state (Fig. 3d). Before shelling the lifetime of ZrO_2:Eu nanoparticles is biexponential with a slower component of 2.7 ± 0.1 ms and a fast component of 1.2 ± 0.1 ms, further confirming the different europium environments. After shelling the decay is monoexponential with a lifetime of 5.3 ± 0.1 ms, an unprecedented result for nanoparticles with such a high doping percentage.[1]

3. Conclusions

It is possible to shell epitaxially zirconia and europium-doped zirconia cores with a protective layer of crystalline zirconium or hafnium oxide. Moreover, upon shelling, europium dopants feature a more uniform coordination environment and a longer photoluminescence lifetime, indicating the suppression of non-radiative pathways. These results[1] initiate zirconium and hafnium oxide hosts as alternatives for the established $NaYF_4$ systems.

Acknowledgements

The author thanks the SNSF Eccelenza funding scheme (project number: 194172).

Received: January 28, 2025

[1] C. Seno, N. Reichholf, F. Salutari, M. C. Spadaro, Y. P. Ivanov, G. Divitini, A. Gogos, I. K. Herrmann, J. Arbiol, P. F. Smet, J. De Roo, *J. Am. Chem. Soc*. **2024**, *146*, 20550, https://doi.org/10.1021/jacs.4c05037.

[2] D. Van den Eynden, R. Pokratath, J. De Roo, *Chem. Rev*. **2022**, *122*, 10538, https://doi.org/10.1021/acs.chemrev.1c01008.

[3] U. Diebold, *Sur. Sci. Rep*. **2003**, *48*, 53, https://doi.org/10.1016/S0167-5729(02)00100-0.

[4] R. N. Patil, E. C. Subbarao, *J. Appl. Crystallogr*. **1969**, *2*, 281, https://doi.org/10.1107/S0021889869007217.

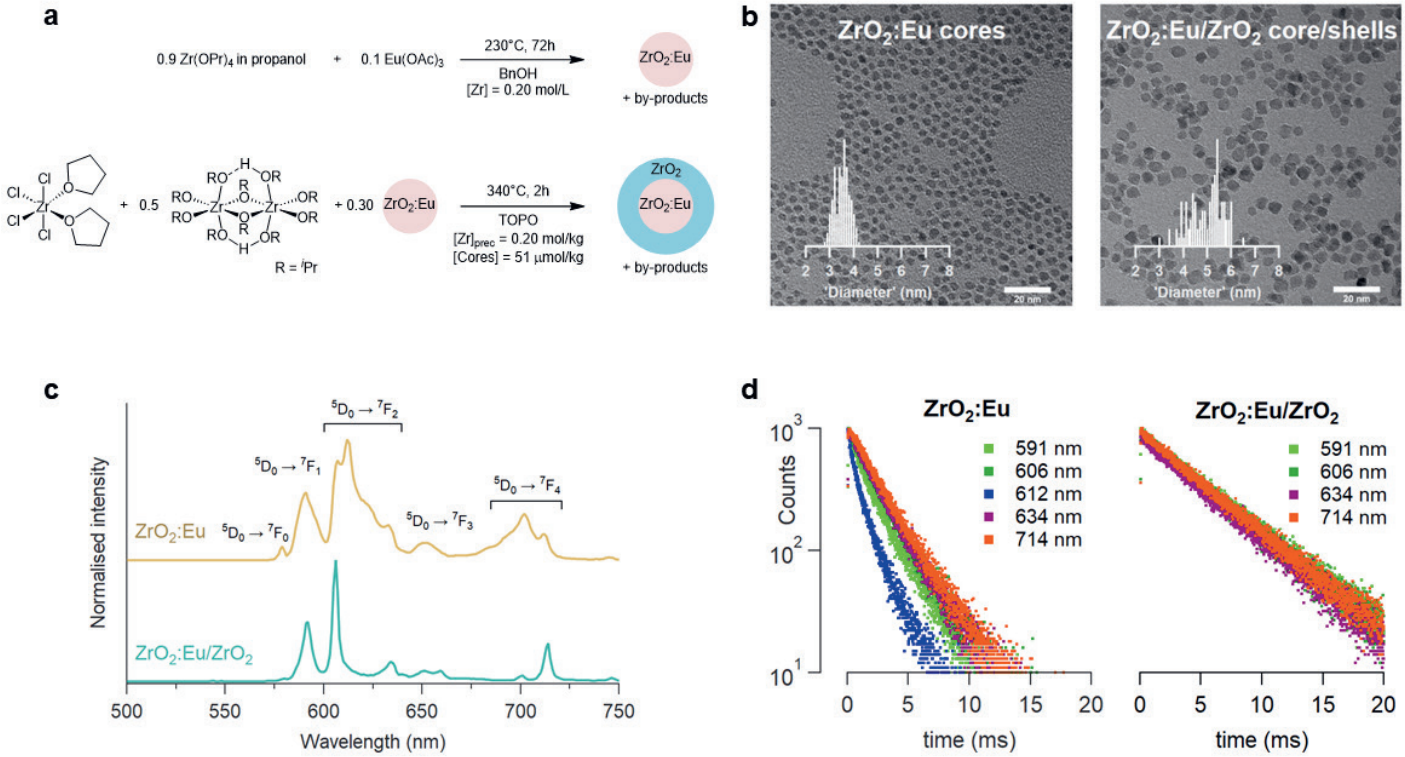

Fig. 3. a) Synthetic procedures to obtain ZrO_2:Eu and ZrO_2:Eu/ZrO_2 core/shell nanocrystals, b) bright-field TEM images of ZrO_2:Eu cores and ZrO_2:Eu/ZrO_2 core/shells, with the histograms based on more than 100 particles, c) photoluminescence emission spectra, and d) lifetime decays of ZrO_2:Eu cores and ZrO_2:Eu/ZrO_2 core/shells. The spectra were collected at room temperature in cyclohexane with an absorbance of 0.1 at 238 nm. Reprinted with permission from ref. [1].

[5] L. Kavan, M. Grätzel, S. Gilbert, C. Klemenz, H. Scheel, *J. Am. Chem. Soc.* **1996**, *118*, 6716, https://doi.org/10.1021/ja954172l.
[6] P. Tao, Y. Li, R. W. Siegel, L. S. Schadler, *J. Appl. Polym. Sci*. **2013**, *130*, 3785, https://doi.org/10.1002/app.39652.
[7] C. Liu, T. J. Hajagos, D. Chen, Y. Chen, D. Kishpaugh, Q. Pei, *ACS Appl. Mater. Interfaces* **2016**, *8*, 4795, https://doi.org/10.1021/acsami.6b00743.
[8] K. De Keukeleere, P. Cayado, A. Meledin, F. Vallès, J. De Roo, H. Rijckaert, G. Pollefeyt, E. Bruneel, A. Palau, M. Coll, *Adv. Electron. Mater*. **2016**, *2*, 1600161, https://doi.org/10.1021/acs.chemmater.7b04580.
[9] J. Wang, S. Choudhary, J. De Roo, K. De Keukeleere, I. Van Driessche, A. J. Crosby, S. S. Nonnenmann, *ACS Appl. Mater. Interfaces* **2018**, *10*, 4824, https://doi.org/10.1021/acsami.7b17376.
[10] S. Maiti, T. Ohlerth, N. Schmidt, S. Aussen, R. Waser, U. Simon, S. Karthuser, *J. Phys. Chem. C* **2022**, *126*, 18571, https://doi.org/10.1021/acs.jpcc.2c06303.
[11] O. Carp, C. L. Huisman, A. Reller, *Progr. Solid State Chem*. **2004**, *32*, 33, https://doi.org/10.1016/j.progsolidstchem.2004.08.001.
[12] H. A. Macleod, 'Thin-film optical filters', **2010**, https://doi.org/10.1201/9781420073034 .
[13] M. Anpo, T. Shima, S. Kodama, Y. Kubokawa, *J. Phys. Chem*. **1987**, *91*, 4305, https://doi.org/10.1021/j100300a021.
[14] A. L. Linsebigler, G. Lu, J. T. Yates Jr, *Chem. Rev*. **1995**, *95*, 735, https://doi.org/10.1021/cr00035a013.
[15] A. Hagfeldt, M. Grätzel, *Acc. Chem. Res*. **2000**, *33*, 269, https://doi.org/10.1021/ar980112j.
[16] M. Grätzel, *J. Sol-Gel Sci. Technol*. **2001**, *22*, 7, https://doi.org/10.1023/A:1011273700573.
[17] B. O'Regan, M. Grätzel, *Nature* **1991**, *353*, 737, https://doi.org/10.1038/353737a0.
[18] S. Cao, S. Zhang, T. Zhang, J. Y. Lee, *Chem. Mat*. **2018**, *30*, 4838, https://doi.org/10.1021/acs.chemmater.8b02196.
[19] L. De Trizio, R. Buonsanti, A. M. Schimpf, A. Llordes, D. R. Gamelin, R. Simonutti, D. J. Milliron, *Chem. Mat*. **2013**, *25*, 3383, https://doi.org/10.1021/cm402396c.
[20] A. Chakraborty, G. H. Debnath, N. R. Saha, D. Chattopadhyay, D. H. Waldeck, P. Mukherjee, *J. Phys. Chem. C* **2016**, *120*, 23870, https://doi.org/10.1021/acs.jpcc.6b08421.
[21] Y. Liu, S. Zhou, D. Tu, Z. Chen, M. Huang, H. Zhu, E. Ma, X. Chen, *J. Am. Chem. Soc*. **2012**, *134*, 15083, https://doi.org/10.1021/ja306066a.
[22] I. Villa, C. Villa, A. Monguzzi, V. Babin, E. Tervoort, M. Nikl, M. Niederberger, Y. Torrente, A. Vedda, A. Lauria, *Nanoscale* **2018**, *10*, 7933, https://doi.org/10.1039/C8NR00724A.
[23] C. LeLuyer, M. Villanueva-Ibañez, A. Pillonnet, C. Dujardin, *J. Phys. Chem. A* **2008**, *112*, 10152, https://doi.org/10.1021/jp803339n.
[24] J. Tang, J. Fabbri, R. D. Robinson, Y. Zhu, I. P. Herman, M. L. Steigerwald, L. E. Brus, *Chem. Mat*. **2004**, *16*, 1336, https://doi.org/10.1021/cm049945w.
[25] R. D. Robinson, J. Tang, M. L. Steigerwald, L. E. Brus, I. P. Herman, *Phys. Rev. B* **2005**, *71*, 115408, https://doi.org/10.1103/PhysRevB.71.115408.
[26] J. Tang, F. Zhang, P. Zoogman, J. Fabbri, S. W. Chan, Y. Zhu, L. E. Brus, M. L. Steigerwald, *Adv. Funct. Mater*. **2005**, *15*, 1595, https://doi.org/10.1002/adfm.200500050.
[27] S. W. Depner, N. D. Cultrara, K. E. Farley, Y. Qin, S. Banerjee, *ACS Nano* **2014**, *8*, 4678, https://doi.org/10.1021/nn501632d.
[28] J. Wang, H. P. Li, R. Stevens, *J. Mater. Sci*. **1992**, *27*, 5397, https://doi.org/10.1007/BF00541601.
[29] I. M. Iskandarova, A. A. Knizhnik, E. A. Rykova, A. A. Bagatur'yants, B. V. Potapkin, A. A. Korkin, *Microelectron. Eng*. **2003**, *69*, 587, https://doi.org/10.1016/S0167-9317(03)00350-2.
[30] J. Joo, T. Yu, Y. W. Kim, H. M. Park, F. Wu, J. Z. Zhang, T. Hyeon, *J. Am. Chem. Soc*. **2003**, *125*, 6553, https://doi.org/10.1021/ja034258b.
[31] R. Pokratath, L. Lermusiaux, S. Checchia, J. P. Mathew, S. R. Cooper, J. K. Mathiesen, G. Landaburu, S. Banerjee, S. Tao, N. Reichholf, *ACS Nano* **2023**, *17*, 8796, https://doi.org/10.1021/acsnano.3c02149.
[32] R. Pokratath, D. Van den Eynden, S. R. Cooper, J. K. Mathiesen, V. Waser, M. Devereux, S. J. Billinge, M. Meuwly, K. M. Jensen, J. De Roo, *JACS Au* **2022**, *2*, 827, https://doi.org/.1021/jacsau.1c00568.
[33] T. Ohlerth, H. Du, T. Hammoor, J. Mayer, U. Simon, *Small Sci.* **2024**, 2300209, https://doi.org/10.1002/smsc.202300209.
[34] K. De Keukeleere, S. Coucke, E. De Canck, P. Van Der Voort, F. Delpech, Y. Coppel, Z. Hens, I. Van Driessche, J. S. Owen, J. De Roo, *Chem. Mat*.**2017**, *29*, 10233, https://doi.org/10.1021/acs.chemmater.7b04580.
[35] A. L. Efros, L. E. Brus, *ACS Nano* **2021**, *15*, 6192, https://doi.org/10.1021/acsnano.1c01399.

License and Terms

The definitive version of this article is the electronic one that can be found at https://doi.org/10.2533/chimia.2025.228